

E5-2002-55

Lubomir Alexandrov

**PRIME NUMBER SEQUENCES
AND MATRICES GENERATED
BY COUNT ARITHMETIC FUNCTIONS**

1 Introduction

Count arithmetic functions for different prime sets can be assigned to *the archaic mathematical reality*.

Nevertheless, the generated by them prime sequences, named *Eratosthenes progressions*, became known only in recent years ([1], sequences A007097, A063502, A064110 in [2]).

The Eratosthenes progression possesses a common formation law of its elements (an inner prime number distribution law) the realization of which is based on a multiple use of the Eratosthenes sieve [3] (Figure 1).

The derivation of Eratosthenes progressions and their systematic investigation are urgent for a solution of the old problem of the strange (nonasymptotic) behaviour of primes, i.e., of the function behaviour

$$d(n) = p(n+1) - p(n), \quad n = 1, 2, \dots, \bar{n},$$

where $p(n)$ is the n th prime and \bar{n} is a sufficiently large natural number.

The inner prime number distribution law can be applied mostly in mathematics itself, for example, when constructing new geometric concepts in arithmetic.

Following Alain Connes ([4] pp. 208–209), it can be supposed that the strange behaviour of primes will reflect itself in the new geometry sought for understanding quantum gravity.

In biochemistry, the strange behaviour of primes can manifest itself in the laws of formation and functioning of large molecules, from 10^3 -atomic insulin and hemoglobin up to $3 \cdot 10^5$ -atomic proteins and enzymes.

In this paper, the general statement of the problem for derivation of Eratosthenes progressions is given and their basic properties are presented. The general results are applied to the sequence of primes itself

$$P = \{2, 3, 5, 7, 11, \dots\} = \{p(n)\}_{n=1,2,\dots}$$

as well as to the following, related to P , subsequences:

$$M = \mathbb{N} \setminus P = \{4, 6, 8, 9, \dots\} = \{m(n)\}_{n=1,2,\dots} \text{ the set of composite numbers;}$$

$$T = \{(p(n), p(n+1)) : p(n+1) = p(n) + 2, n = 1, 2, \dots\} = \{t(n)\}_{n=1,2,\dots} \\ \text{the set of twins;}$$

$T_1 = \{p(n) : (p(n), p(n+1)) \in T, n = 1, 2, \dots\} = \{t_1(n)\}_{n=1,2,\dots}$ the set of first elements of twins;

$T_2 = \{p(n+1) : (p(n), p(n+1)) \in T, n = 1, 2, \dots\} = \{t_2(n)\}_{n=1,2,\dots}$ the set of second elements of twins;

$T_3 = T_1 \cup T_2 = \{3, 5, 7, 11, 13, 17, 19, \dots\}$ the set of twin elements;

$S = P \setminus T_3 = \{2, 23, 37, 47, 53, \dots\}$ the set of isolated primes[2], A007510;

$D_{6n-1} = \{6n-1 \in P : n = 1, 2, \dots\} = \{5, 11, 17, \dots\}$ the Dirichlet set of primes of kind $6n-1$;

$D_{6n+1} = \{6n+1 \in P : n = 1, 2, \dots\} = \{7, 13, 19, \dots\}$ the Dirichlet set of primes of kind $6n+1$, and

$T_4 = \{t(n) : (t_1(n) + t_2(n))/2 = 6 \cdot q, q \in P\}$ the set of twins with minimal average [6], p. 15.

The sets T, T_1, T_2, T_3, S and T_4 will further be supposed to be infinite.

In this paper, a number of infinitesimal properties of Eratosthenes progression for primes is presented, namely, the distribution laws of the progression elements, a ζ -function for the progression and its connection with the Riemann ζ -function.

The main result of this paper consists in the proposed plane-spiral arithmetic model in place of the linear (Cartesian) one.

The real semiaxis \mathbb{R}_+^1 in the new geometric model is isometrically mapped into a *logarithmic spline-spiral* on the plane \mathbb{R}^2 in such a way that the Eratosthenes rays, not intersecting each other, cross the spiral at the primes.

The spiral arithmetic allows one to interpret in a new way the basic count function $\pi(x)$, the Ω -theorem of Littlewood, and also gives an arithmetic interpretation of the distribution in natural series of all kinds of clusters of primes (see [5], for example) and twin pairs, in particular.

The basic object in the spiral geometry is a spider-web W_n composed of spiral and Eratosthenes rays intersecting it in which the number of rotations n infinitely increases.

The web W_n consists of embedded *concave-convex trapezoids* of primes

MESM

1	31	11	5	3	2	1	61	18	91
2	32						62		92
3	33						63		93
4	34						64		94
5	35						65		95
6	36						66		96
7	37	12					67	19	97
8	38						68		98
9	39						69		99
10	40						70		100
11	41	13	6				71	20	101
12	42						72		102
13	43	14					73	21	103
14	44						74		104
15	45						75		105
16	46						76		106
17	47	15					77		107
18	48						78		108
19	49						79	22	109
20	50						80		110
21	51						81		111
22	52						82		112
23	53	16					83	23	113
24	54						84		114
25	55						85		115
26	56						86		116
27	57						87		117
28	58						88		118
29	59	17	7	4			89	24	119
30	60						90		120
									121
									122
									123
									124
									125
									126
									127
									128

Multiple Eratosthenes Sieve Machine

Figure 1:

with a characteristic formation law. This law is a direct consequence of the inner prime number distribution law.

The plane \mathbb{R}^2 is considered as a *mosaic* composed of *elementary concave-convex trapezoids*.

The web W_n geometrically select primes, and also all kinds of linear and plane configurations of primes.

2 Splitting theorem of infinite sequences of primes

2.1 Basic definitions

Let sets $A \subset \mathbb{N}$ and $B \subset \mathbb{N}$ with the properties

$$A \cap B = \emptyset, \quad (1)$$

$$A \cup \overline{B} = \mathbb{N}, \quad (2)$$

where $\overline{B} = \{1\} \cup B$, be given.

Let the arithmetic function

$$g(n) : \mathbb{N} \rightarrow A$$

generate (denote) the n th element $a(n) \in A$.

Then *the count recurrent law*

$$\varepsilon_{a(0)}^+ : a(n+1) = g(a(n)), n = 0, 1, 2, \dots, a(0) \in \mathbb{N} \quad (3)$$

determines an A -count progression $\varepsilon_{a(0)}^+$ and an A -count ray

$$r_{a(0)} = \{a(n) : a(n+1) = g(a(n)), n = 0, 1, 2, \dots, a(0) \in \mathbb{N}\}.$$

Together with the function $g(n)$, its inverse function, the n th number of element $a(n) \in A$, is also uniquely determined (in a purely arithmetical sense it is a count function)

$$g_{-1}(a) : A \rightarrow \mathbb{N}.$$

The functions $g(n)$ and $g_{-1}(a)$ are strictly monotonic and satisfy the equalities

$$g(g_{-1}(a)) = a, \quad g_{-1}(g(n)) = n.$$

By means of $g(n)$ and $g_{-1}(a)$ the compositions

$$g_n(a(0)) = \underbrace{g(\dots g(a(0)) \dots)}_n,$$

$$g_{-n}(a(n_1)) = \underbrace{g_{-1}(\dots g_{-1}(a(n_1)) \dots)}_n, \quad \text{with } n \leq n_1.$$

are introduced.

The compositions satisfy the equalities

$$g_{n_1}(g_{n_2}(a(0))) = g_{n_1+n_2}(a(0)), \quad n_1, n_2 \geq 1,$$

$$g_{-n_1}(g_{n_2}(a(0))) = g_{n_2-n_1}(a(0)), \quad 1 \leq n_1 \leq n_2.$$

An extension of the A -count Eratosthenes progression $\varepsilon_{a(0)}^+$ with negative numbers $\varepsilon_{a(0)}^- = -\varepsilon_{a(0)}^+$ leads to the infinite cyclic group

$$\varepsilon_{a(0)} = \varepsilon_{a(0)}^- \cup \{a(0)\} \cup \varepsilon_{a(0)}^+, \quad g_{-n}(a(0)) = -g_n(a(0)), \quad n > 0 \quad (4)$$

under composition $g_n(a(0))$, with a *depth* $n \in \mathbb{Z}$ and *generator* $a(0) \in \overline{B}$.

Two elements from $\varepsilon_{a(0)}$ interact under the composition rule

$$g_{n_1}(a(0)) \odot g_{n_2}(a(0)) = g_{n_1}(g_{n_2}(a(0))) = g_{n_1+n_2}(a(0)), \quad n_1, n_2 \in \mathbb{Z}. \quad (5)$$

2.2 Basic assertion and its consequences

The following assertion holds about the splitting of the set A into a denumerable number of denumerable subsets with a common law of formation of its elements (3).

A -split theorem. *For any sets A and B with properties (1) and (2) there hold equalities*

$$\bigcap_{a(0) \in \overline{B}} r_{a(0)} = \emptyset,$$

$$\bigcup_{a(0) \in \overline{B}} r_{a(0)} = A.$$

The A -split theorem leads to a matrix representation of the sequences A and \mathbb{N} . The elements of these matrices possess peculiar properties, invariant with respect to the kind of set A .

Corollary 1. *There exists a one-to-one mapping*

$$\overline{\varphi}(a(0)) : \overline{B} \rightarrow {}^2A = \{r_{a(0)}\}_{a(0) \in \overline{B}} \equiv \{a_{\mu\nu}\}_{\mu, \nu=1,2,\dots} \quad (6)$$

(2A denotes the matrix representation of the elements A).

From (6) a matrix representation to the natural numbers

$${}^2\mathbb{N} = \|\overline{B} \quad {}^2A\|, \quad (7)$$

where $\overline{B} = \text{Column}\{a_{\mu 0}\}_{\mu=1,2,\dots}$, also follows.

The matrices 2A and ${}^2\mathbb{N}$ shall be called *mesm*-matrices.

In the case when $A = P$ and $B = M$ an example of the left upper corner of the matrix ${}^2\mathbb{N}$ ([6], pp. 18–22) is given in Appendix 1.

Corollary 2. *The rows of matrices ${}^2\mathbb{N}$ are isomorphic to the row r_1 with respect to the mapping*

$$\Psi(g_n(1)) : g_n(1) \rightarrow g_{-n}(g_n(1)) \rightarrow a(0) \rightarrow g_n(a(0)), \quad a(0) \in \overline{B}, \quad a(0) > 1.$$

The columns of the matrix 2A are isomorphic to the column \overline{B} with respect to the mapping

$$\varphi(a(0)) : a(0) \rightarrow g_n(a(0)), \quad a(0) \in \overline{B}.$$

In the case $A = P$ and $B = M$ Figure 2 illustrates the isomorphisms indicated in Corollary 2.

In Figure 2, a one-to-one correspondence between *rooted trees* and elements of \mathbb{N} , proposed by F. Göbel [7], is used (see the 1th row of Figure 2).

From the A -split theorem a consequence follows which reveals the arithmetical nature of the fine structure of the set A element distribution among the natural numbers.

Let $g_{-1}(n', n'')$, $n', n'' \in \mathbb{N}$ denote the number of elements A inside the interval (n', n'') .

Corollary 3. *For the matrix $[\overline{B} \quad {}^2A]$ elements the following equalities*

hold:

$$\left. \begin{aligned} g_{-1}(a_{\mu 0}, 0) &= a_{\mu 1} - 1, \quad \mu = 1, 2, \dots, \\ g_{-1}(a_{\mu_1 \nu_1}, a_{\mu_2 \nu_2}) &= |a_{\mu_1(\nu_1-1)} - a_{\mu_2(\nu_2-1)}| - 1, \\ \mu_i, \nu_i &\geq 1, \quad i = 1, 2. \end{aligned} \right\} \quad (8)$$

3 Application of the A-split theorem to special cases of A and B

3.1 About new A-count progressions

In the cases when A and B take usual values, the law (3) generates known A -count progressions. So, for example, at $A = \{\text{even}\}$ and $B = \{\text{odd}\}$ a generating function is of kind $g(a(n)) = 2a(n) - 1$ and in this case $\varepsilon_2^+ = \{2, 3, 5, 9, 17, 33, 65, 129 \dots\}$ is a Pisot sequence ([2], A000051).

New A -progressions occur when the behaviour of A elements among natural numbers is unknown and it cannot be considered probabilistic. Besides the sequences of primes P , all subsequences of P , in the formation of which the Eratosthenes sieve combines with an additional deterministic filter $f(n)$ (this is the formation rule of the considered subsequence), should also be considered belonging to this class. The set of these subsequences shall be denoted by \mathcal{E}_f .

The Dirichlet theorem about the existence of infinite primes of the kind $\alpha n + \beta$ (an additional filter) for arbitrary coprime numbers α and β shows that \mathcal{E}_f is infinite.

In particular, we have inclusions $T_1, T_2, T_3, S \in \mathcal{E}_f, \quad D_{\alpha n \pm 1} \in \mathcal{E}_f, \alpha = 4, 6$.

For all elements \mathcal{E}_f there exists a $mesm_f$ -process which is analogous to the process represented in Figure 1. From the A -split theorem it follows that for every $A_f \in \mathcal{E}_f$ and $B_f = \mathbb{N} \setminus A_f$ there exists an $mesm_f$ -matrix $[B_f \ ^2A_f]$.

As a result of a $mesm$ -transition $A_f \rightarrow \ ^2A_f$, the elements of the rows $\ ^2P, \ ^2T_1, \ ^2T_2, \ ^2T_3, \ ^2S$ and $\ ^2D_{\alpha n \pm 1} (\alpha = 4, 6)$ already will be distributed according to the *inner law* (3), which now should be understood as a specific *self-smoothing* (only with respect to the rows $\ ^2A_f$) of the irregularities in the appearance of the elements A_f in the natural series.

3.2 Basic case: $\mathbf{A} = \mathbf{P}$ and $\mathbf{B} = \mathbf{M}$

The upper left corner of the matrix 2P and its extension to the matrix ${}^2\mathbb{N}$ are represented in Appendix 1. The P -split theorem has been proved inductively in [6], pp. 4–8.

The first elements of the first rows of the matrix 2P were primarily determined *by hand* by means of *MESM* (Figure 1). In such a way the law (3) with $g(n) = p(n)$ was discovered [3].

The extension of the matrix 2P rows on negative primes according to the rules (4), (5) leads to infinite cyclic groups under composition $p_n(a(0))$, $n \in \mathbb{Z}$ with a generator $a(0)$. An example of such a group is the set

$$\varepsilon_4 = \{\dots, -p_n(4), \dots, -59, -17, -7, 4, 7, 17, 59, \dots, p_n(4), \dots\}.$$

A part of 2P , represented in Appendix 1, has been computed by means of **Mathematica** function **NestList[Prime, a(0), n]**.

The row elements of the matrix $[\overline{M} \quad {}^2P]$ determine new subsets of natural numbers

$$N_m = \{p_{n_1}^{\alpha_1}(m) \dots p_{n_k}^{\alpha_k}(m) : \forall n_i, \alpha_i \in \mathbb{N}, i = 1, 2, \dots, k, \forall k \in \mathbb{N}\}, m \in \overline{M} :$$

$$N_1 = \{2, 3, 2^2, 5, 2 \cdot 3, 2^3, 3^2, 2 \cdot 5, 11, 2^2 \cdot 3, 3 \cdot 5, 2^4, \dots\},$$

$$N_4 = \{7, 17, 7^2, 59, 7 \cdot 17, 277, 17^2, 7^3, 7 \cdot 59, 7^2 \cdot 17, 1787, 7^4, \dots\},$$

$$N_6 = \{13, 41, 13^2, 179, 13 \cdot 41, 1063, 41^2, 13^3, 13^2 \cdot 41, \dots\}, \dots$$

According to Corollary 2, the behaviour of composite numbers reflects on the behaviour of the elements of the columns of the matrix 2P .

On the other hand, the structure of the set M depends on the structure of the set of primes because M can be represented as a chain of α_μ -element segments (where $\alpha_\mu = d(\mu) - 1$) from consequent composite numbers

$$\overline{m}_\mu(\alpha_\mu) = \{p(\mu) + 1, p(\mu) + 2, \dots, p(\mu + 1) - 1\}, \quad \mu = 2, 3, \dots$$

$$(\overline{m}_2(1) = \{4\}, \overline{m}_3(1) = \{6\}, \overline{m}_4(3) = \{8, 9, 10\}, \dots).$$

The segments are connected in a whole set M by means of *ghost primes* $\omega_\mu = \langle p(\mu) \rangle$ ($\omega_2 = \langle 3 \rangle$, $\omega_3 = \langle 5 \rangle$, $\omega_4 = \langle 7 \rangle$, ...).

The Eratosthenes progressions $\{\varepsilon_m^+\}_{m \in \overline{M}}$ (i.e., rows of the matrix 2P) conform to the inner prime number distribution law

$$a(n + 1) = p(a(n)) = p_n(a(0)), \quad n = 0, 1, 2, \dots, a(0) \equiv m \in \overline{M}, \quad (9)$$

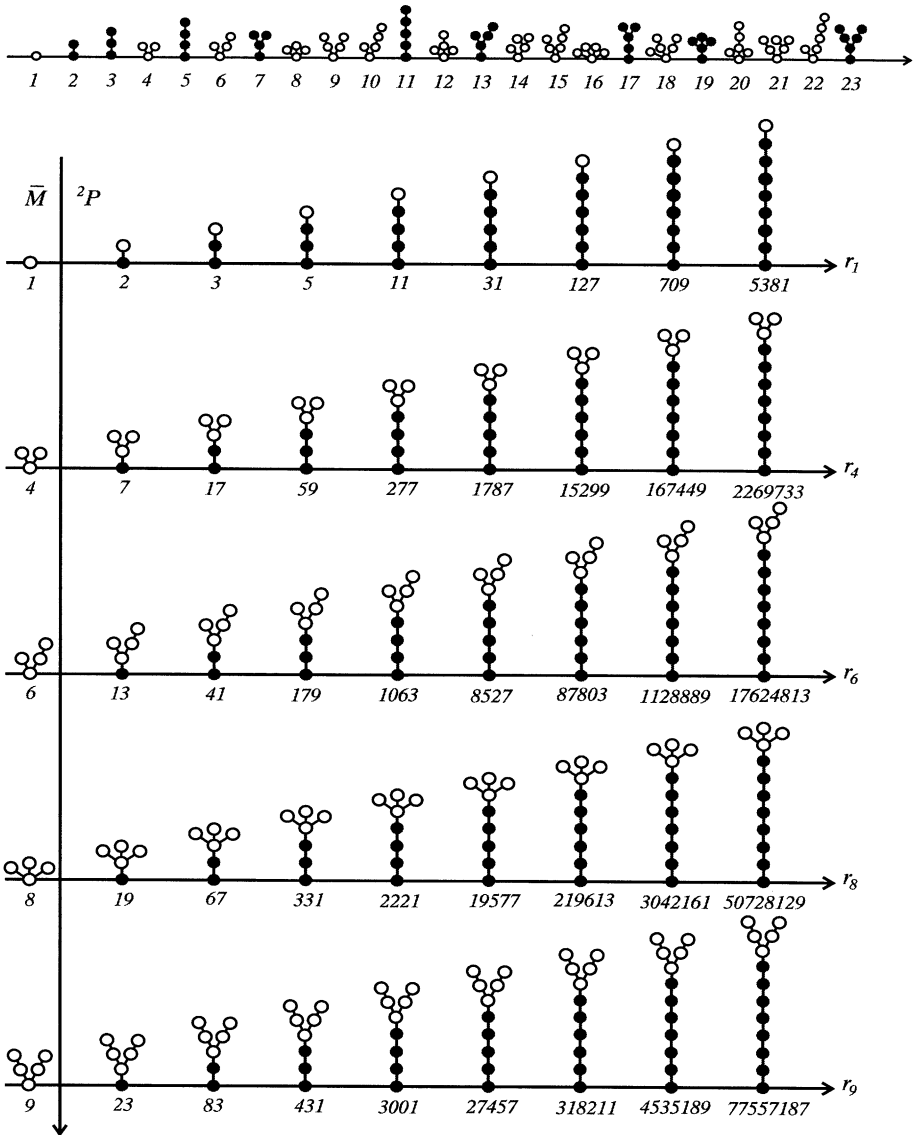


Figure 2: "MESM & F. Göbel" forest of rooted trees

but the deviation of the rows 2P between each other, (i.e., the distribution of primes in the columns of 2P), again persists dependent of the oddish behaviour of primes.

The main information left out of the inner law (9) is reflected in the structure of the first matrix 2P column

$$P_1 = \text{column}[p_{11}, p_{21}, \dots, p_{\mu 1}, \dots].$$

The following assertion about the P_1 structure is valid.

P_1 -structure theorem. *Mapping $\varphi : a(0) \rightarrow p_{\mu 1}$ defines a correspondence between segments of composite numbers $\bar{m}_\mu(\alpha_\mu)$ and clusters of α_μ -successive primes*

$$c_\mu(\alpha_\mu) = \{p_1(p(\mu) + 1), p_1(p(\mu) + 2), \dots, p_1(p(\mu + 1) - 1)\} \subset P$$

in the cases $\alpha_\mu \geq 3$, and separate primes $p_1(p(\mu) + 1)$ in the cases $\alpha_\mu = 1$. At their ends the clusters are complemented by the ghost images up to prime number segments

$$\bar{c}_\mu(\alpha_\mu) = \{p_1(\langle p(\mu) \rangle), c_\mu(\alpha_\mu), p_1(\langle p(\mu + 1) \rangle)\}.$$

Herewith the equality $P = \bigcup_{\mu=1}^{\infty} \bar{c}_\mu(\alpha_\mu)$ is fulfilled.

The next theorem about twin pairs $t(\bar{n}) = (t_1(\bar{n}), t_2(\bar{n})) \in T$, $\bar{n} = 1, 2, \dots$ is also justified.

Twin Theorem. *For each pair $t(\bar{n})$ at least one of the elements $t_1(\bar{n})$ or $t_2(\bar{n})$ belongs to the first column P_1 of the matrix 2P .*

The mapping $\varphi^{-1} : p_{\mu 1} \rightarrow m_\mu$ defines a correspondence between pairs with both elements on P_1 (u -twin) and pairs of subsequent elements of some segment $\bar{m}_{\bar{\mu}}(\alpha_{\bar{\mu}}) \subset M$ with $\alpha_{\bar{\mu}} \geq 3$.

For a pair with one element $t_1(\bar{n})$ (or $t_2(\bar{n})$) on P_1 (b -twin) the mapping $\varphi^{-1} : p_{\mu 1} \rightarrow m(\mu)$ associates $t_1(\bar{n})$ with the element $p(n) + 1$, or the element $p(n + 1) - 1$ of some segment $\bar{m}_{\bar{\mu}}(\alpha_{\bar{\mu}}) \subset M$ at $\alpha_{\bar{\mu}} \geq 3$, or with the element of some one-element segment $\bar{m}_{\bar{\mu}}(1) \subset M$.

The mapping $\varphi^{-1} : p_{\mu_1 \nu_1} \rightarrow p_{\mu_1(\nu_1-1)}$, $\nu_1 \geq 2$ relates the second element $t_2(\bar{n})$ (or $t_1(\bar{n})$) to one of the ghosts $\langle p(\mu) \rangle \equiv p_{\mu_1(\nu_1-1)}$, or $\langle p(\mu + 1) \rangle \equiv p_{\mu_1(\nu_1-1)}$.

Let us also note the following properties of the matrix 2P rows and columns:

- q1)** The differences $d_m(n) = p_{(n+1)}(m) - p_n(m)$, $n = 1, 2, \dots$, $m \in \overline{M}$ monotonically increase under the estimate

$$d_m(n) > p_n(m)(\ln p_n(m) - 1)$$

unlike the difference $d(n)$ whose behaviour only at first glance may seem to be a chaotical one [8];

- q2)** The sequences $\tau(s, m) = \sum_{n=1}^{\infty} \frac{1}{p_n^s(m)}$ converge for all $m \in \overline{M}$ and $s \geq 1$.

Note especially the convergence of the sum $\tau(1, m)$ ([6], p. 10) when the sum $\sum_{n=1}^{\infty} \frac{1}{p(n)}$ diverges;

- q3)** An analogue of the Euler identity holds

$$\zeta(s, m) = \sum_{n \in N_m} \frac{1}{n^s} = \prod_{n=1}^{\infty} \left(1 - \frac{1}{p_n^s(m)}\right)^{-1}, \quad m \in \overline{M}, s \geq 1;$$

- q4)** The Riemann function $\zeta(s) = \sum_{n=1}^{\infty} \frac{1}{n^s}$, $s \in \mathcal{Q}'$ can be represented by the functions $\zeta(s, m)$

$$\zeta(s) = \prod_{m \in \overline{M}} \zeta(s, m);$$

- q5)** The asymptotic law for the primes and the simplified Riemann formula for $\pi(x)$ give an opportunity to find approximately $p_{n+1}(m)$, $m \in \overline{M}$, by solving the equations with respect to x

$$Li(x) = p_n(m), \tag{10}$$

$$R(x) = p_n(m), \tag{11}$$

$$\text{where } Li(x) = \int_0^x \frac{ds}{\ln(s)}, \quad R(x) = \sum_{k=1}^{\infty} \frac{\mu(k)}{k} Li(x^{1/k})$$

and $\mu(k)$ is a Möbius function;

q6) There exists an approximate formula

$$n = \int_{\alpha}^{p_n(\beta)} \frac{ds}{s \ln \ln s} + \varepsilon(n, \beta), \quad (12)$$

where $\alpha = 11$ and $\beta = 1$, $n > 4$ for r_1 , $\alpha = 7$ and $\beta = 4$ for r_4 and $\alpha = \beta = m$ for the other rays r_m .

The absolute error $|\varepsilon|$ for the part of the matrix $[\overline{M}^2 P]$ in Appendix 1 is not greater than 0.2 when n is small and 0.06 when n is large.

Formula (12) is a *prime number distribution law* of the rays 2P .

On Figure 3, the behaviour of the function (12) is presented for the ray r_9 ;

q7) The number μ of element $p_{\mu n}$ in the matrix 2P column

$$P_n = \text{column}[p_{1n}, p_{2n}, \dots, p_{\mu n}, \dots]$$

is determined by the asymptotic formula

$$\mu \sim m - \int_2^m \frac{ds}{\ln s}. \quad (13)$$

This is the column 2P *prime number distribution law*.

In order to use (12) and (13) it is necessary to know the composite number m .

3.3 About other A-count progressions

Applying the A-split theorem in the cases

$$A = T_1 \text{ and } B_1 = T_2 \cup M,$$

$$A = S \text{ and } B_2 = M \cup T_3,$$

$$A = D_{6n-1} \text{ and } B_3 = M \cup D_{6n+1} \cup \{2, 3\}$$

и

$$A = D_{6n+1}, B_4 = M \cup D_{6n-1} \cup \{2, 3\},$$

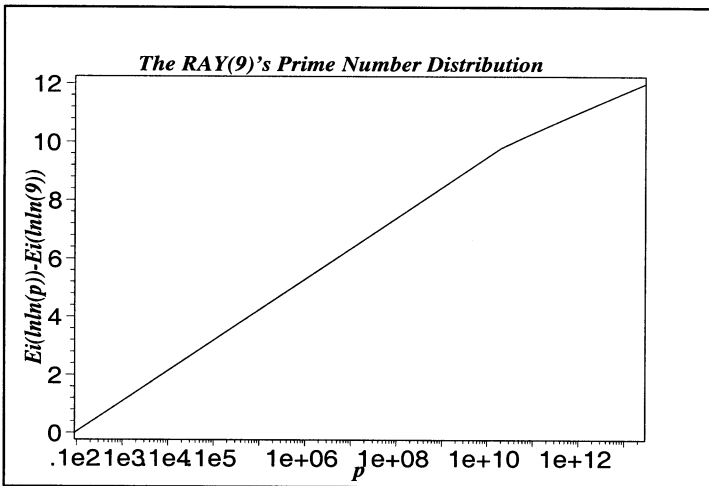


Figure 3:

we can obtain the next $mesm_f$ -matrices of kind (7):

$$[B_1 \ ^2T_1] = \begin{bmatrix} 1 & 3 & 11 & 137 & 5639 & 641129 & 152921807 \dots \\ 2 & 5 & 29 & 641 & 44381 & 7212059 & \dots \\ 4 & 17 & 239 & 12161 & 1583927 & \dots & \\ 6 & 41 & 1151 & 93251 & 16989317 & \dots & \\ 7 & 59 & 1931 & 176021 & 35263691 & \dots & \\ 8 & 71 & 2339 & 221201 & 45749309 & \dots & \\ \cdot & \cdot & \cdot & \cdot & \cdot & \dots & \dots \end{bmatrix};$$

$$[B_2 \ ^2S] = \begin{bmatrix} 1 & 2 & 23 & 263 & 2917 & 38639 & 603311 & 11093633 \dots \\ 3 & 37 & 397 & 4751 & 64403 & 1038629 & 19661749 & \dots \\ 4 & 47 & 491 & 5897 & 81131 & 1328167 & 25467419 & \dots \\ 5 & 53 & 557 & 6709 & 93287 & 1541191 & 29778547 & \dots \\ \cdot & \cdot & \cdot & \cdot & \cdot & \cdot & \cdot & \dots \\ 22 & 257 & 2861 & 37799 & 589181 & 10821757 & 230452837 & \dots \\ 24 & 277 & 3079 & 40823 & 640121 & 11807167 & 252480587 & \dots \\ \cdot & \cdot & \cdot & \cdot & \cdot & \cdot & \cdot & \dots \end{bmatrix};$$

$$[B_3 \ ^2D_{6n-1}] = \begin{bmatrix} 1 & 5 & 29 & 263 & 3767 & 76253 & 2049263 & 69633521 \dots \\ 2 & 11 & 83 & 953 & 16223 & 381221 & 11579489 & \dots \\ 3 & 17 & 137 & 1721 & 31883 & 795803 & 25434641 & \dots \\ 4 & 23 & 197 & 2663 & 51803 & 1348961 & 44635001 & \dots \\ 6 & 41 & 419 & 6329 & 135347 & 3808109 & 134441441 & \dots \\ \cdot & \cdot & \cdot & \cdot & \cdot & \cdot & \cdot & \dots \end{bmatrix} ;$$

$$[B_4 \ ^2D_{6n+1}] = \begin{bmatrix} 1 & 7 & 61 & 727 & 12343 & 284083 & 8457367 & 312953941 \dots \\ 2 & 13 & 109 & 1429 & 26113 & 642937 & 20262883 & 787318099 \dots \\ 3 & 19 & 181 & 2539 & 49669 & 1291471 & 42627997 & \dots \\ 4 & 31 & 331 & 5011 & 105277 & 2908753 & 10144807 & \dots \\ 5 & 37 & 397 & 6211 & 133633 & 3761239 & 132710947 & \dots \\ \cdot & \cdot & \cdot & \cdot & \cdot & \cdot & \cdot & \dots \end{bmatrix} .$$

The matrices $[B_1 \ ^2T_1]$, $[B_2 \ ^2S]$ and $[P \ ^2M]$ were published in [2] as A063502, A064110 and A025003–A025006, respectively. Matrices $[B_3 \ ^2D_{6n-1}]$ and $[B_4 \ ^2D_{6n+1}]$ are the new ones.

The new *mesm_f*-matrices can be obtained also for the Euler primes of the kind $n^2 + n + 41$ ($r_1 = \{41, 1847, 1573316, \dots\}$), and for the Hardy-Littlewood primes of the kind $H_{n^2+1} = \{n^2 + 1 \in P : n = 1, 2, \dots\}$, where at $B_5 = \mathbb{N} \setminus H_{n^2+1}$ we have

$$[B_5 \ ^2H_{n^2+1}] = \begin{bmatrix} 1 & 2 & 5 & 101 & 746497 & 286961228404901 \dots \\ 3 & 17 & 7057 & 11424189457 \dots \\ 4 & 37 & 44101 & 637723627777 \dots \\ 6 & 197 & 3496901 \dots \\ 7 & 257 & 6421157 \dots \\ \cdot & \cdot & \cdot & \dots \end{bmatrix} .$$

All pointed out *mesm_f*-matrices are not studied. In particular, an analogue of the distribution laws (12) and (13) has not been found for them with the exception of the matrix $[P \ ^2M]$ for which an analogue of the law (13) is known. However, the common Corollaries 2 and 3 of the *A*-split theorem remain valid for them.

4 Logarithmic geometry of primes on the plane

4.1 The Prime Number Spider Web (PNSW) Hypothesis

One of the main applications of *the prime number distribution law* (9) consists in constructing the plane spiral arithmetic model. Let

$$\mathcal{L}_f = \{\rho(\theta) = (f(\theta))^\theta : f(\theta) \in C^1[0, \infty), f(\theta) \geq 1, 0 \leq \theta < \infty\}$$

denote a class of logarithmic spirals with an arc length

$$\lambda(0, \theta) = \int_0^\theta (f(x))^x \left(\left(\ln f(x) + \frac{x f'(x)}{f(x)} \right)^2 + 1 \right)^{1/2} dx.$$

The plane spiral model is based on the following PNSW–hypothesis [3].

Conjecture 1. *On the plane \mathbb{R}^2 there exists a unique spiral $\bar{\rho}(\theta) \in \mathcal{L}_f$ and the corresponding to it sets of angles*

$$\{\theta_{mn}\}_{m \in \overline{M}}, n = 1, 2, \dots, \quad \theta_{mn'} < \theta_{mn''} \text{ at } n' < n''$$

such that the following conditions are fulfilled:

(i) $\lambda(0, \theta_{mn}) = p_n(m), n = 1, 2, \dots, m \in \overline{M};$

(ii) *the primes $p_n(m), n = 1, 2, \dots$ lie on the same ray $\ell_m \subset R^2$ with a positive direction corresponding to increasing n ;*

(iii) *two arbitrary rays ℓ_{m_1} and $\ell_{m_2}, m_1, m_2 \in \overline{M}$ do not intersect each other and are nonparallel.*

4.2 A Logarithmic spline–spiral

Under the substitution $f(\theta) = e^{\cot \varphi}$, \mathcal{L}_f turns into a one–parametric family of logarithmic spirals

$$\mathcal{L}_\varphi = \left\{ \rho_\varphi = e^{(\cot \varphi)\theta} : 0 < \varphi < \frac{\pi}{2}, 0 \leq \theta < \infty \right\}$$

with an arc length

$$\lambda(0, \theta) = \frac{1}{\cos \varphi} \left(e^{(\cot \varphi)\theta} - 1 \right). \quad (14)$$

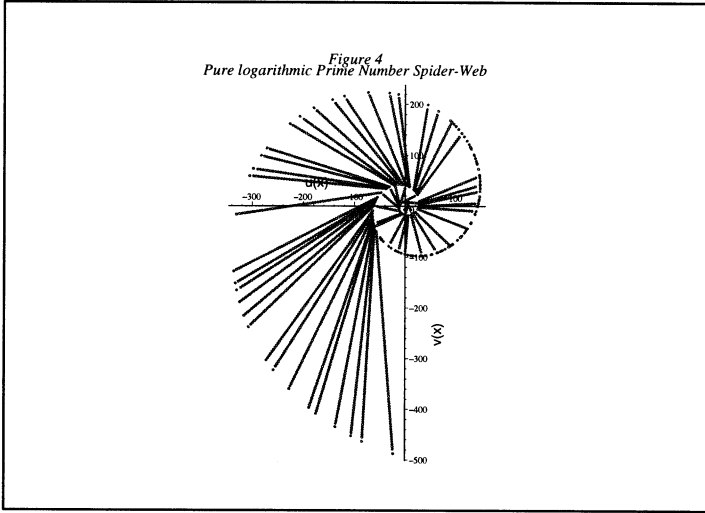


Figure 4: *Pure logarithmic prime number spider web*

Now the required by the PNSW-hypothesis, sets of angles with respect to m and n , according to the condition (i), are given by the formula

$$\theta_{mn} = \tan \varphi \ln(p_n(m) \cos \varphi + 1)).$$

For simple logarithmic spirals the conditions (ii) and (iii) of the PNSW-hypothesis are not fulfilled, because the equation [3]

$$S_{n_1 n_2}(x) + S_{n_2 n_3}(x) + S_{n_3 n_1}(x) = 0, \quad (15)$$

where

$$S_{\alpha\beta}(x) = (p_\alpha(m)x + 1)(p_\beta(m)x + 1) \sin \left(\sqrt{\frac{1}{x^2} - 1} \ln \frac{(p_\alpha(m)x + 1)}{(p_\beta(m)x + 1)} \right)$$

cannot be satisfied with the same value $x = \cos \varphi$ for any triplets $(p_{n_1}(m), p_{n_2}(m), p_{n_3}(m))$ from any ray r_m , $m \in \overline{M}$.

Nevertheless, the solution (15) for all the denoted prime triplets from all rays of the matrix in Appendix 1 shows that x remains in a sufficiently narrow interval $I_x = (0.202, 0.326)$ with an average $\bar{x} \approx 0.264$, to which there corresponds a value $\bar{\varphi} \approx 74.69^\circ$. On Figure 4, a pure-logarithmic web is presented where only the condition (i) is fulfilled.

This result stimulates us to search for a solution of the PNSW-hypothesis in the class of logarithmic spline-spirals (LSS):

$$\rho_{s_1}(\theta) = e^{s_1(\theta)},$$

$$s_1(\theta) = \begin{cases} \alpha_{i+1}\theta + \beta_{i+1}, & \theta_i \leq \theta \leq \theta_{i+1} \quad 0 \leq i \leq k-1, \\ \alpha_{i-1}\theta_{i-1} + \beta_{i-1} = \alpha_i\theta_{i-1} - \beta_i = 0, & 2 \leq i \leq k, \end{cases}$$

where the 1st degree spline $s_1(\theta)$ is defined on an irregular set

$$\Delta_k : 0 = \theta_0 < \theta_1 < \theta_2 < \dots < \theta_{k-1} < \theta_k,$$

with a number $k \geq 3$ of subintervals $[\theta_i, \theta_{i+1}]$, $0 \leq i \leq k-1$ which increases with the number of rotations n of the web $W_n(P)$.

The unknowns in the spiral $\rho_{s_1}(\theta)$ are both the knots of the set Δ_k and the spline-spiral coefficients of the elements $e^{\alpha_i\theta + \beta_i}$

$$\{\alpha_i, \theta_i, \beta_i\}_{i=1,2,\dots,k}.$$

They are determined from the conditions of the PNSW-hypothesis with regard for the initial condition

$$e^{\alpha_1\theta_0 + \beta_1} = 1 \implies \beta_1 = 0. \quad (16)$$

For arbitrary $x \in \mathbb{R}_+^1$ there exists a unique $p(k_x) \in P$ such that $p(k_x - 1) \leq x < p(k_x)$, and the isometric transformation $x \in \mathbb{R}_+^1$ into \mathbb{R}^2 determined by the condition (i) of the PNSW-hypothesis, acquires an explicit form

$$h_{\rho_{s_1}}(x) : \mathbb{R}_+^1 \rightarrow \lambda(0, \theta_x) = p(k_x - 1) + \sqrt{1 + \frac{1}{\alpha_{k_x}^2}} e^{\beta_{k_x}} \left(e^{\alpha_{k_x}\theta_x} - e^{\alpha_{k_x}\theta_{k_x-1}} \right), \quad (17)$$

where

$$0 \leq x < \infty, \quad \theta_x = \frac{1}{\alpha_{k_x}} \ln E(x),$$

$$E(x) = \frac{\alpha_{k_x}}{\sqrt{1 + \alpha_{k_x}^2}} e^{-\beta_{k_x}(x - p(k_x - 1))} + e^{\alpha_{k_x}\theta_{k_x-1}}, \quad p(0) = 0.$$

The points $(u_x, v_x) \in \rho_{s_1}(\theta) \subset \mathbb{R}^2$, which correspond to the numbers $x \in \mathbb{R}_+^1$, have the Euler and Cartesian coordinates, respectively:

$$\rho(\theta_x) = e^{\alpha_{k_x} \theta_x + \beta_{k_x}} = e^{\beta_{k_x}} \ln E(x), \quad \theta_x = \frac{1}{\alpha_{k_x}} \ln E(x) \quad (18)$$

and

$$u_x = \rho(\theta_x) \cos(\theta_x), \quad v_x = \rho(\theta_x) \sin(\theta_x). \quad (19)$$

The first plane spiral isometric to the semi-axis \mathbb{R}_+^1 was constructed in [9]. The computer investigation of the function $d(n) = p(n+1) - p(n)$, $n = 1, 2, \dots$ begins with the appearance of this paper.

4.3 About constructing the webs W_n

Attempts to construct the spiral $\rho_{s_1}(\theta)$ under the PNSW-hypothesis for a given n lead to a denial of some number k^0 of starting primes because of the difficulty in fulfilling the condition (ii) around the origin of \mathbb{R}^2 (condition (i) remains valid for the missed primes). In this paper, the case $k^0 = 11$ is considered, i.e., instead of the rays r_1, r_4, r_6, r_8, r_9 and r_{10} , the truncated rays $\bar{r}_1, \bar{r}_4, \bar{r}_8, \bar{r}_9$ and \bar{r}_{10} obey the condition (ii) and these rays start with 127, 59, 41, 87, 83 and 109, respectively.

According to (16), to the first element $e^{\alpha_1 \theta}$ ($0 \leq \theta \leq \theta_1$) of the spiral ρ_{s_1} there corresponds a real segment $[0, p(k^0 + 1)]$.

The rotations W_n are taken into account from the ray

$$r_{12} = \{37, 157, 919, 7193, \dots\}$$

in the direction counter-clockwise.

At first, $\rho_{s_1}^{(3)}$ and W_3 are constructed on the basis of the first 3 elements of the first 25 rays $\bar{r}_1, \bar{r}_4, \dots, r_{36}$ plus the fourth element of the ray r_{12} .

The satisfaction of the conditions (i), (ii) of the PNSW-hypothesis with regard to (16), leads to a solution of a nonlinear system (W_3 -system) of 228 equations with respect to 228 unknowns

$$\{\alpha_i, \theta_i, \beta_i\}_{i=1,2,\dots,76}.$$

The W_3 -system is solved providing that 304 inequalities, caused by the condition (iii), are satisfied.

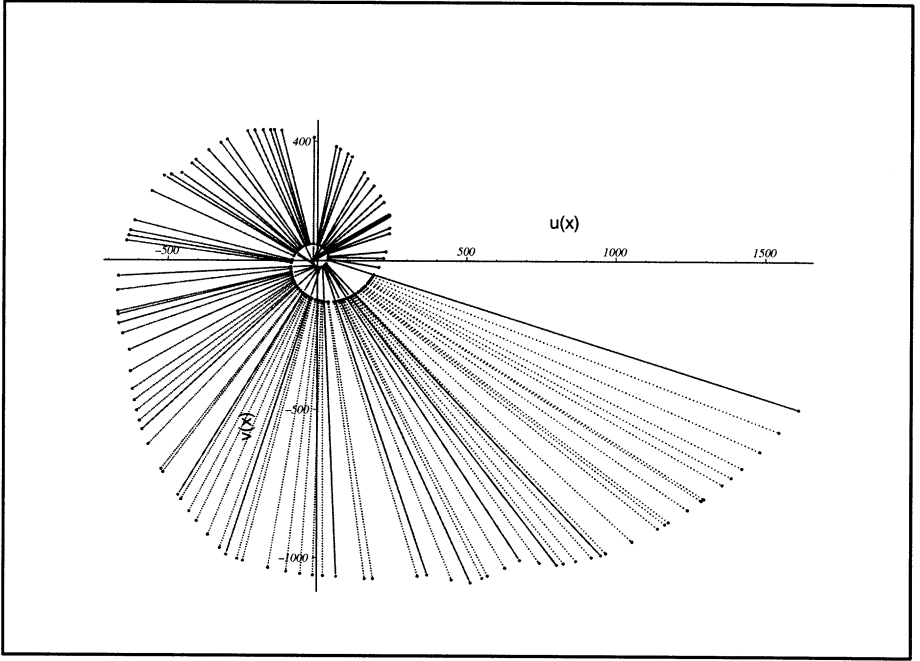


Figure 5: *3-rotation prime number spider web.* The thick black line denotes the initial ray r_{12} . The direction of rotation is counter-clockwise

All 832 primes up to the number 7193, which remain unused in the construction of the W_3 -system ($p_{-1}(7193) = 919$; $11 + (25 \times 3 + 1) + 832 = 919$), are placed by the Cartesian coordinates (19) on the 2nd and 3rd rotation of $\rho_{s_1}^{(3)}$.

The building up of new rotations $n > 3$ on $\rho_{s_1}^{(3)}$ is reduced to the subsequent solution of 3×3 nonlinear systems of equations.

Both solvability and uniqueness of the mentioned infinite set of nonlinear systems are an analytical interpretation of the content of the PNSW-hypothesis.

A desire to avoid the solution of the W_3 -system leads to a construction of approximations \widetilde{W}_3 , \widetilde{W}_4 and \widetilde{W}_5 in which the first two turns are constructed as a simple spiral from \mathcal{L}_φ . The subsequent rotations are constructed as LSS. In these webs $\varphi = 74.18896^\circ$.

The web \widetilde{W}_3 fairly well illustrates the main properties of the prime

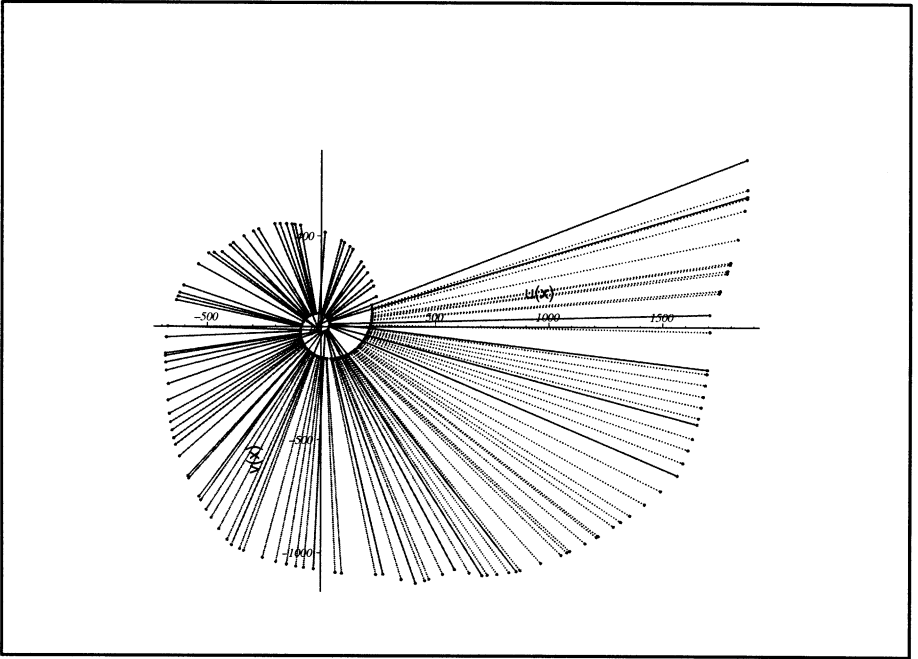


Figure 6: 3-rotation prime number spider web with full 3rd turn

number spider webs, and the web \widetilde{W}_4 shows the possibility of continuing the construction of higher rotations. The web \widetilde{W}_3 is created for a generation of initial approximations to a solution of the W_3 -system. It also illustrates the defects of the approximated webs.

The web \widetilde{W}_3 is presented in Figure 5. It is constructed on the basis of 211 primes: 3 numbers from each of the first 20 rays from \bar{r}_1 to r_{30} , 2 numbers from 5 rays from r_{32} to r_{36} and 2 numbers from each of the 71 rays from r_{38} to r_{126} ($3 \cdot 20 + 2 \cdot 5 + 2 \cdot 71 = 211$); 147 of these primes are placed on the 2nd and the 3rd rotations by means of coordinates (19).

The web \widetilde{W}_3 does not have a complete 3rd rotation, ending in the number 5381 from the ray \bar{r}_1 and not reaching number 7193 from the initial ray r_{12} , marked in Figures 5 and 9 by a thick black line. To simplify the figure, 498 primes remaining until $p_{-1}(5381) = 709$ ($709 - 211 = 498$) are not placed on the 3rd rotation.

The web \widetilde{W}_3 with a full 3rd rotation is represented in Figure 6. It is built on the basis of 255 primes: 3 from the first 25 rays from \bar{r}_1 to r_{36} and

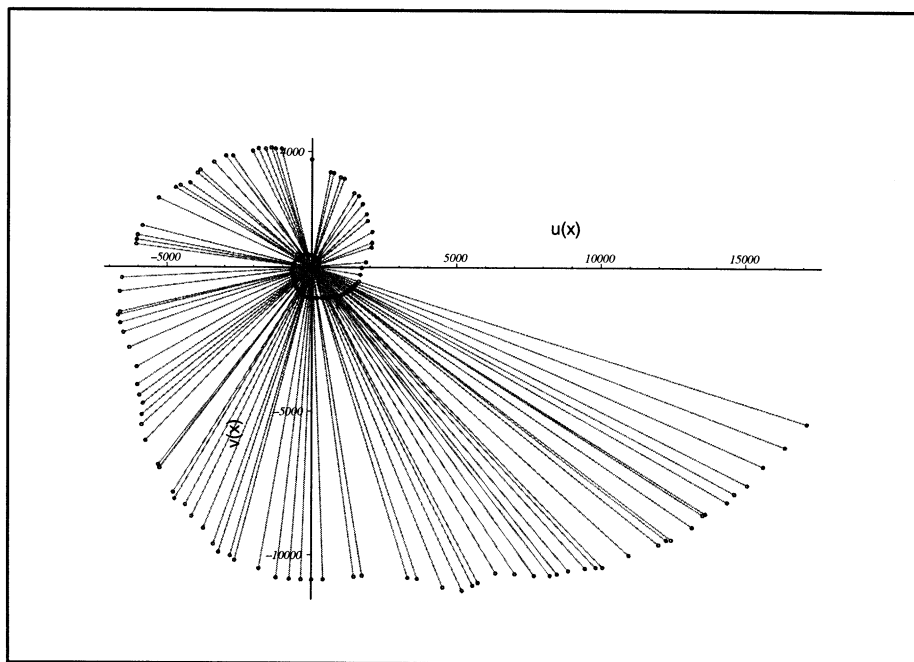


Figure 7: \widetilde{W}_4 -rotation prime number spider web. In the center of the picture one can see the web \widetilde{W}_3

2 from 90 rays from r_{38} to r_{151} ($3 \cdot 25 + 2 \cdot 90 = 255$); 180 of these primes are placed on the 2nd and the 3rd rotations by means of coordinates (19).

To simplify the figure, 664 primes ($919 - 255 = 664$) remaining up to $p_{-1}(7193) = 919$ are not placed on the 3rd rotation.

At the end of the 3rd rotation \widetilde{W}_3 , (at the transition of the logarithmic spiral into LSS) a unessential *qualitative defect* shows up between numbers 877 from r_{36} and 919 from r_{12} . The pointed defect obstructs the exact sewing of the spirals between the numbers 6823 and 7193 from the corresponding rays r_{36} and r_{12} . This defect is removable by solving the \widetilde{W}_3 -system.

The web \widetilde{W}_4 , represented in Figure 7, is obtained from the web \widetilde{W}_3 by adding on the 4th rotation as LSS. In this building, 96 primes are used: 4 elements of the rays from \bar{r}_1 to r_{30} , 3 elements of the rays from r_{32} to r_{36} and 4 elements of the rays from r_{38} to r_{126} ($20 + 5 + 71 = 96$). By means of 116 primes the LSS-units $e^{\alpha_i \theta_i} + \beta_i$, $i = 1, 2, \dots, 116$ are determined by

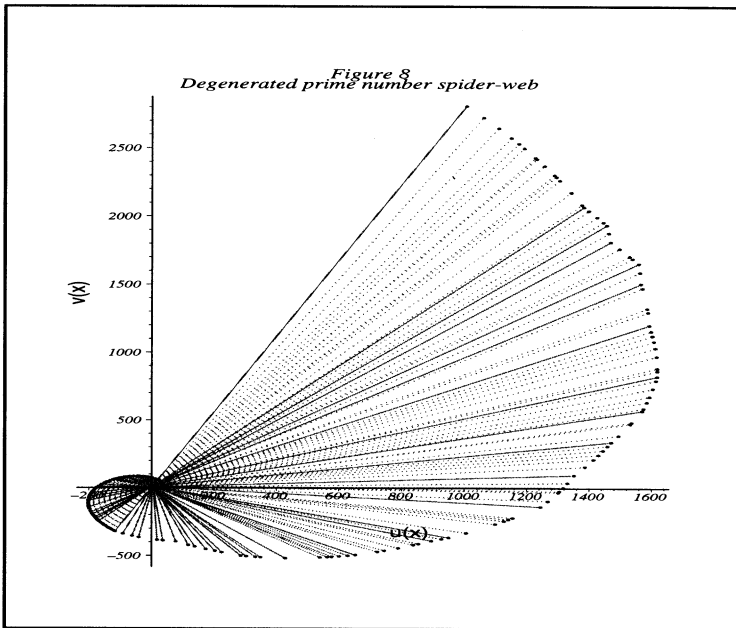


Figure 8: *Degenerated prime number spider web*

solving a 3×3 nonlinear system 116 times with respect to 348 unknowns α_i, θ_i and β_i : 94 times exactly and 22 times approximately. The cases of inexact solutions result in unessential distortions of the condition (ii) for 22 rays (in the diagrams of \widetilde{W}_3 and \widetilde{W}_4 those distortions are not seen).

A variety of possibilities for constructing the PNSW-hypothesis is illustrated by web \widetilde{W}_{deg} (Figure 8), in which the condition (ii) is violated in the following way: the rays lie on straight lines, but the subsequent segments of the rays have the opposite directions. In \widetilde{W}_{deg} , the same primes are used as in \widetilde{W}_3 .

4.4 Web formation rules and properties

Satisfying the PNSW-hypothesis, the conditions of \widetilde{W}_3 and \widetilde{W}_4 fix the individual peculiarities of the behaviour of primes around the origin of \mathbb{R}^2 as concrete systems of embedded trapezoids confined between the rays $\ell_{p_{\mu 1}}$ and $\ell_{p_{(\mu+k)1}}$, $k \geq 1$. For example, the trapezoid t_{19} , confined between the

rays ℓ_{113} and ℓ_{127} (Figure 9), is one of the nineteen *3-rotation embedded trapezoids (3RET)* of the web \widetilde{W}_3 .

From a P_1 -structure theorem it follows that

- q8)** The elements of the clusters $c_{\alpha_\mu}(\alpha_\mu)$ (they and only they) become the starts of new rays on the spiral $\rho_{s_1}(\theta)$.

Let a cluster

$$c_\mu(k) = \{p_{\mu 1}, p_{(\mu+1)1}, \dots, p_{(\mu+k)1}\}.$$

lie on the ν th rotation of the spiral $\rho_{s_1}^{(n)}(\theta)$. On the $(\nu + q)$ th rotation to it there correspond the primes $\{p_q(p_{(\mu+i)1})\}_{i=0,1,\dots,k}$.

The PNSW-hypothesis shows that

- q9)** The geometric figure on \mathbb{R}^2 , confined between the arcs $(p_{\mu 1}, p_{(\mu+k)1})$ and $(p_q(p_{\mu 1}), p_q(p_{(\mu+k)1}))$ by the spiral ρ_{s_1} and the segments $|p_{\mu 1}, p_q(p_{\mu 1})|$, $|p_{(\mu+k)1}, p_q(p_{(\mu+k)1})|$ of the rays $\ell_{p_{\mu 1}}$ and $\ell_{p_{(\mu+k)1}}$, is the convex-concave trapezoid

$$z(\nu, \mu, k, q) = [(p_{\mu 1}, p_{(\mu+k)1}), (p_q(p_{\mu 1}), p_q(p_{(\mu+k)1}))].$$

The trapezoids of the type $z(\nu, \mu, 1, 1)$ are *elementary trapezoids (or holes)* to W_n . For example

$$z(1, 19, 1, 1) = [(113, 127), (617, 709)]$$

is an elementary W_2 -trapezoid (Figure 10).

Let the primes $p_{\mu 1}, p_{(\mu+k)1} \in c_\mu(\alpha_\mu)$, $\alpha_\mu \geq 3$, $0 \leq k \leq \alpha_\mu$ lie on the ν th rotation of the spiral $\rho_{s_1}^{(n)}$. On the $(\nu + 1)$ th rotation, to them there corresponds the cluster $c_{\mu_1}(\alpha_{\mu_1}) = \{p_{\mu_1 1}, p_{(\mu_1+1)1}, \dots, p_{(\mu_1+\alpha_{\mu_1})1}\}$ with a length $\alpha_{\mu_1} = p_{(\mu+k)1} - p_{\mu 1} - 1$, according to Corollary 3.

From the conditions of the PNSW-hypothesis there stems the following rule for formation of 3RET:

- q10)** On the plane \mathbb{R}^2 the following equalities hold

$$z(\nu + 1, \mu_1, \alpha_{\mu_1} + 1, 1) = \bigcup_{i=0}^{\alpha_{\mu_1}} z(\nu + 1, \mu + i, 1, 1), \quad (20)$$

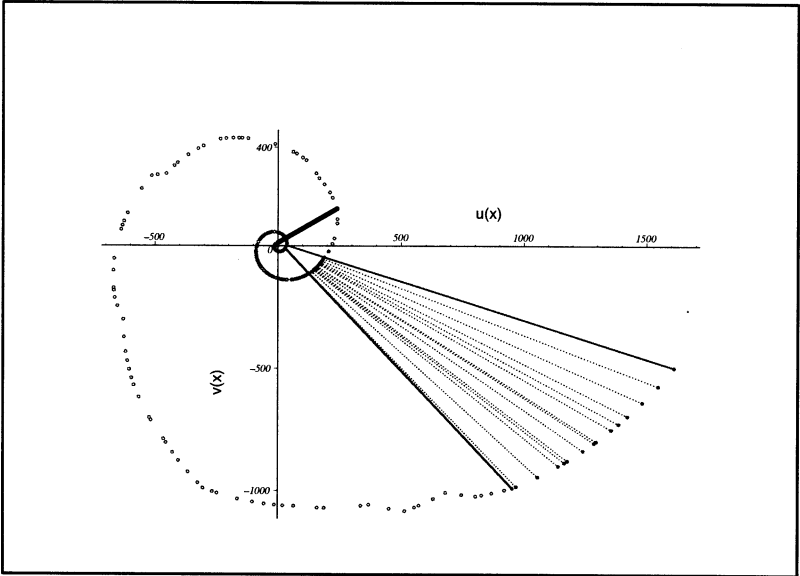


Figure 9: \mathcal{R} -rotation system of embedded trapezoids $3RET_{19} = z(1, 19, 1, 2) = [(113, 127), (4549, 5381)]$. The thick black line defines the initial ray r_{12} . The direction of rotation is counter-clockwise

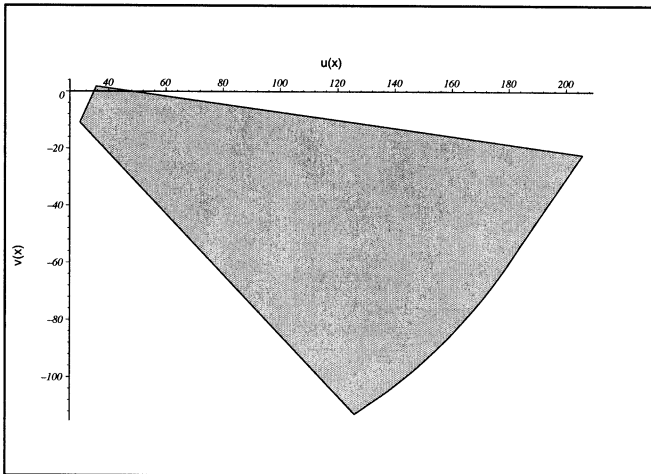


Figure 10: The elementary trapezoid $z_{19} = z(1, 19, 1, 1) = [(113, 127), (617, 709)]$

$$z(\nu, \mu, 1, 2) = z(\nu, \mu, 1, 1) \cup z(\nu + 1, \mu_1, \alpha_{\mu_1} + 1, 1). \quad (21)$$

Equalities (20) and (21) can be regarded as those between the areas (the sign \cup changes to $+$).

Let us apply the rule for formation of 3RET to $3RET_{19}$. Using the matrix from Appendix 1, we obtain

$$3RET_{19} = [(113, 127), (617, 709)] \cup [(617, 619), (4549, 4567)] \cup \\ [(619, 631), (4567, 4663)] \cup \dots \cup [(701, 709), (5281, 5381)].$$

In this example $\nu = 1$, $\mu = 30$, $\alpha_{\mu_1} = 127 - 113 - 1 = 13$. The starts of the newly-appeared rays on the second rotation are

$$p(114) = 619, \quad p(115) = 631, \quad p(116) = 641, \quad p(117) = 643, \\ p(118) = 647, \quad p(119) = 653, \quad p(120) = 659, \quad p(121) = 661, \\ p(122) = 673, \quad p(123) = 677, \quad p(124) = 683, \quad p(125) = 691, \quad \text{and} \\ p(126) = 701.$$

q₁₁) The rule for formation of 3RET shows that 3RET is a mosaic of $\alpha_{\mu_1} + 1$ elementary trapezoids which are grouped in the direction of the ray $\ell_{p_{\mu_1}}$ in the following way:

the first is the elementary trapezoid

$$z[(p_{\mu_1}, p_{(\mu+1)_1}), p_1(p_{\mu_1}), p_1(p_{(\mu+1)_1})],$$

followed by the composite trapezoid

$$z[(p_1(p_{\mu_1}), p_1(p_{(\mu+\alpha_{\mu_1})_1}), (p_2(p_{\mu_1}), p_2(p_{(\mu+\alpha_{\mu_1})_1}))].$$

The elements (elementary trapezoids too) of the last one cause in total $\mu_2 = p_1(p_{(\mu+\alpha_{\mu_1})_1}) - p_1(p_{\mu_1}) - 1$ new rays on the $(\nu + 2)$ th rotation, to which again the 3RET formation rule is applied for obtaining α_{μ_2} new composite trapezoids located between the 3rd and 4th rotations of W_n .

Under the condition of the PNSW-hypothesis the process of growth of the initial 3RET is unlimited and leads to the formation of a class $(\ell_{p_{\mu_1}}, \ell_{p_{(\mu+1)_1}})$ -trapezoids containing an unlimited number of different elementary trapezoids.

q12) Let *mitos* denote a closed geometric figure locked between the arc $(p(12), p_1(12))$ of the spiral ρ_{s_1} and the segment $|p(12), p_1(12)|$ of the ray r_{12} . Then the plane \mathbb{R}^2 can be represented as a mosaic of the initial $k(k^0)$ -classes of embedded trapezoids ($k(11)=25$):

$$\mathbb{R}^2 = \bigcup_{i=1}^{k(k^0)} (\ell_{p(k^0+i)}, \ell_{p(k^0+i+1)}) \cup \textit{mitos}.$$

Inside the *mitos* the starts of the first few rays can intersect each other, i.e., be in a mitosis status.

Properties q_{10}), q_{11}) and q_{12}) are generalized into the property q_{13} .

q13) The plane \mathbb{R}^2 is representable as a mosaic (in the theoretical-set sum sense) of all the prime-numerical elementary trapezoids and *mitos*.

q14) The PNSW-hypothesis leads to the geometric interpretation of $\pi(x)$:

$$\pi(p_\nu(m)) = p_{\nu-1}(m) = \lambda(0, p_{\nu-1}(m)), \quad \nu \geq 2, m \in \overline{M}. \quad (22)$$

Equalities (22) allow one to interpret geometrically the Ω -theorem of Littlwood and Theorem 1 from [10], where for setting the real values and in particular the values of $Li(x)$ again the transformation $h_{\rho_{s_1}}(x)$ and coordinates (19) are used.

The geometric interpretation of the twin theorem consists in determination of the laws for appearance of u- and b-twins on W_n :

q15) u-twins appear on W_n in the following cases:

a) as starts of new rays $\ell_{p_{\mu 1}}$ and $\ell_{p_{(\mu+1)1}}$ on the 1st rotation 3RET which on the 2nd rotation cause 1 new ray $\ell_{p((p_{\mu 1}+p_{(\mu+1)1})/2)}$. Then 3RET is composed of 3 elementary trapezoids.

Examples:

$$\begin{aligned} \overline{m}_8(3) &\rightarrow (\ell_{71}, \ell_{73}) \rightarrow \ell_{359}, \\ \overline{m}_9(5) &\rightarrow (\ell_{101}, \ell_{103}) \rightarrow \ell_{557}, \\ \overline{m}_{11}(5) &\rightarrow \begin{cases} (\ell_{137}, \ell_{139}) \rightarrow \ell_{787}, \\ (\ell_{149}, \ell_{151}) \rightarrow \ell_{863}; \end{cases} \end{aligned}$$

b) as a pair of subsequent primes on the 2nd rotation of 3RET

Examples on the 2nd turn of the trapezoid $z(1, 19, 1, 2)$ (Figure 9):

$$\overline{m}_{30}(13) \rightarrow \begin{cases} (\ell_{641}, \ell_{643}) \rightarrow \ell_{4783}, \\ (\ell_{659}, \ell_{661}) \rightarrow \ell_{4937}. \end{cases}$$

q₁₆) One of the elements of b-twin $(t_1(\overline{n}), t_2(\overline{n}))$ lies on the existing ray $\ell_{p_q(p_{\mu_1})}$, $q \geq 1$, but the other element is a start of a new ray $\ell_{p_{\mu_2}}$:

$$t_1(\overline{n}) \equiv p_q(p_{\mu_1}), t_2(\overline{n}) \equiv p_{\mu_2} - \text{right twin};$$

$$t_1(\overline{n}) \equiv p_{\mu_2}, t_2(\overline{n}) \equiv p_q(p_{\mu_1}) - \text{left twin}$$

In such a way the b-elementary trapezoid

$$[(p_q(p_{\mu_1}), p_{\mu_2}), (p_{q+1}(p_{\mu_1}), p(p_{\mu_2}))]$$

is sewn together to the right of the ray $\ell_{p_{\mu_1}}$, and trapezoid

$$[(p_{\mu_2}, p_q(p_{\mu_1})), (p(p_{\mu_2}), p_{q+1}(p_{\mu_1}))]$$

to the left of the ray $\ell_{p_{\mu_1}}$.

Examples: the trapezoid $[(617, 619), (4549, 4567)]$ is sewn to the right of the ray ℓ_{113} ($(\ell_{617}, \ell_{619}) \rightarrow \ell_{4561}$);

the trapezoid $[(857, 859), (6653, 6661)]$ is sewn to the left of the ray ℓ_{149} ($(\ell_{857}, \ell_{859}) \rightarrow \ell_{6659}$).

The properties q_{15}) and q_{16}) show the following W_n sewing property

q₁₇) The twin pairs sew uniformly over n the Eratosthenes rays in a unified plane web W_n , $n = 1, 2, \dots$.

5 Conclusion

The study of the inner prime number distribution law remains at the initial stage.

Finally, we shall note how the proof of Conjecture 1 looks like, and we shall find a possibility of its generalization. We should like to indicate possible applications of the proposed, in this paper, approach to a study of the oddish prime number behaviour.

At the first stage of the proof of Conjecture 1 it is necessary to solve the W_3 -system and revise the number k^0 . If the W_3 -system cannot be solved with $k^0 = 11$, then the numbers $k^0 = 10$ and $k^0 = 12$ should be tried.

In the formulation of the W_3 -system a function $\tilde{p}(x) \in C^1(0, 10000]$, with a property

$$\tilde{p}(n) = p(n), \quad n = 1, 2, \dots, 1229 \quad (23)$$

is used.

This function can be built up by *the rod spline method* [11] using as a rod the approximation ([12], problem 9.21).

$$\bar{p}(x) = x \left(\ln x + \ln \ln x + \frac{\ln \ln x - 2}{\ln x} - \frac{(\ln \ln x)^2/2 - 3 \ln \ln x - 5.5}{(\ln x)^2} - 1 \right).$$

The searched function will be of the form $\tilde{p}(x) = s_2(x)\tilde{p}(x)$ where $s_2(x)$ is a parabolic spline. At the interpolation points, equalities (23) are fulfilled.

The W_3 -system solvability can first be investigated numerically by using, for example, the program LANCELOT [13].

At the second stage of the proof of Conjecture 1, it is necessary to prove inductively the continuability of the *basic $k(k^0)$ -classes of embedded trapezoids*

$$(\ell_{p_{(k^0+i)_1}}, \ell_{p_{(k^0+i+1)_1}}), \quad i = 1, 2, \dots, k(k^0),$$

as well as the continuability of *the new classes on rotations $n \geq 2$* .

Conjecture 1 can be extended to all *mesm_f*-matrices.

Conjecture 2. *For each matrix $A_f \in \mathcal{E}_f$ there exists LSS-spiral and a web $W_n(A_f)$, satisfying the conditions (i), (ii) and (iii) of the PNSW-hypothesis.*

In the infinite set of webs $\mathbf{w} = \{W_n(A_f) : A_f \in \mathcal{E}_f, n = 1, 2, \dots\}$ it is necessary to introduce an operation *summing webs* @ in such a way that the equalities

$$W_n(S)@W_n(T_1)@W_n(T_2) = W_n(P)$$

and

$$W_n(D_{6n-1})@W_n(D_{6n+1}) = W_n(P),$$

hold, by analogy with the set-theoretical equalities $P = S \cup T_1 \cup T_2$ and $P = D_{6n-1} \cup D_{6n+1} \cup \{2, 3\}$, where $\{2, 3\} \subset \text{mitos}$.

On the whole, the algebraic structures of mesm-matrices $[B_f \ ^2A_f]$, webs $W_n(A_f)$ and the set \mathbf{w} remain unexplored.

The spiral $\rho_{s_1}(\theta)$ length from the PNSW-hypothesis can turn out to be an appropriate *time coordinate* in the description of physical processes taking place in asymmetric and irreversible time.

Indeed, the mapping (17) can be extended also for negative values $x \in (-\infty, 0]$:

$$h_{\rho_{s_1}}(x) : \mathbb{R}_-^1 \rightarrow \lambda(0, \theta_x) = \frac{1}{\cos \varphi} \left(e^{(\cot \varphi)\theta_x} - 1 \right),$$

$$-\infty < x \leq 0, \varphi = \operatorname{arccot}(\alpha_1).$$

In such a way, in the unit circle (inside the domain *mitos*) there remains a finite *negative moustache* with a length

$$\lambda(0, -\infty) = -\frac{1}{\cos \varphi}.$$

Now, the arc length of the spiral $\rho_{s_1}(\theta)$, $-\infty < \theta < \infty$ is split up into three pieces: the length of *the negative moustache*, the finite positive length spiral in the *mitosis* and the infinite arc length corresponding to the semi-axis $[p(k^0 + 1), \infty)$.

The solution of equations (10), (11) provides a motivation for the following hypothesis:

Conjecture 3. *For arbitrary $m \in \overline{M}$ and large n the inequality*

$$|Li(p_{n+1}(m)) - p_n(m)| \leq c_1 \sqrt{p_{n+1}(m)} \ln(p_{n+1}(m)) \quad (24)$$

is fulfilled with a constant c_1 independent of m .

Inequalities (24) result in the common estimate

$$|Li(x) - \pi(x)| < c_2 \sqrt{x} \ln x, \quad c_2 = \text{const.} \quad (25)$$

The proof of inequality (24) is easier than the proof of inequality (25). If estimation (25) leads to the Riemann hypothesis ([14], p.6) that complex solutions of the equations $\zeta(s) = 0$, $s \in \mathcal{C}$ have a form $s = 1/2 + i\gamma_n$, $\gamma_n \in \mathbb{R}$, $n = 1, 2, \dots$, then the inner prime number distribution law (9) will prove to be a new useful tool of the analytical number theory.

Appendix 1

Matrix $[\overline{M}^2P]$

1	2	3	5	11	31
		127	709	5381	52711
		648391	9737333	174440041	3657500101
		88362852307	2428095424619		
		75063692618249...			
4	7	17	59	277	1787
		15299	167449	2269733	37139213
		718064159	16123689073	414507281407	
		12055296811267...			
6	13	41	179	1063	8527
		87803	1128889	17624813	326851121
		7069067389	175650481151	4952019383323...	
8	19	67	331	2221	19577
		219613	3042161	50728129	997525853
		22742734291	592821132889	17461204521323...	
9	23	83	431	3001	27457
		318211	4535189	77557187	1559861749
		36294260117	963726515729	28871271685163...	
10	29	109	599	4397	42043
		506683	7474967	131807699	2724711961
		64988430769	1765037224331	53982894593057...	
12	37	157	919	7193	72727
		919913	14161729	259336153	5545806481
		136395369829	3809491708961...		
14	43	191	1153	9319	96797
		1254739	19734581	368345293	8012791231
		200147986693	5669795882633...		
15	47	211	1297	10631	112129
		1471343	23391799	440817757	9672485827
		243504973489	6947574946087...		
16	53	241	1523	12763	137077
		1828669	29499439	563167303	12501968177
		318083817907	9163611272327...		
18	61	283	1847	15823	173867
		2364361	38790341	751783477	16917026909
		435748987787	12695664159413...		
20	71	353	2381	21179	239489
		3338989	56011909	1107276647	25366202179
		664090238153	19638537755027...		
21	73	367	2477	22093	250751
		3509299	59053067	1170710369	26887732891
		705555301183	20909033866927...		

Appendix 1

Matrix \overline{M}^2P ... Continuation 1.

22	79	401	2749	24859	285191
		4030889	68425619	1367161723	31621854169
		835122557939	24894639811901...		
24	89	461	3259	30133	352007
		5054303	87019979	1760768239	41192432219
		1099216100167	33080040753131...		
25	97	509	3637	33967	401519
		5823667	101146501	2062666783	48596930311
		1305164025929	39510004035659...		
26	101	547	3943	37217	443419
		6478961	113256643	2323114841	55022031709
		1484830174901	45147154715447...		
27	103	563	4091	38833	464939
		6816631	119535373	2458721501	58379844161
		1579041544637	48112275898789...		
28	107	587	4273	40819	490643
		7220981	127065427	2621760397	62427213623
		1692866362237	51702420222709...		
30	113	617	4549	43651	527623
		7807321	138034009	2860139341	68363711327
		1860306318433	56997887937671...		
32	131	739	5623	55351	683873
		10311439	185350441	3898093877	94434956839
		2606906998739	80783250929599...		
33	137	773	5869	57943	718807
		10875143	196100297	4135824247	100450108949
		2773622459039	86127342906779...		
34	139	797	6113	60647	755387
		11469013	207460717	4387715993	106839327589
		2956887579073...			
35	149	859	6661	66851	839483
		12838937	233784751	4973864561	121763369327
		3386468161121...			
36	151	877	6823	68639	864013
		13243033	241568891	5147813641	126206581463
		3514741569337...			
38	163	967	7607	77431	985151
		15239333	280256489	6016014239	148471002899
		4159843299587...			

Appendix 1

Matrix $[\bar{M}^2 P] \dots$ Continuation 2.

39	167	991	7841	80071	1021271
		15837299	291905681	6278569691	155231019913
		4356423418499...			
40	173	1031	8221	84347	1080923
		16827557	311234591	6715304579	166500464477
		4684808232443...			
42	181	1087	8719	90023	1159901
		18143603	337033877	7300206493	181639026043
		5127173445557...			
44	193	1171	9461	98519	1278779
		20137253	376292689	8194134017	204869160779
		5808496248769...			
45	197	1201	9739	101701	1323503
		20890789	391182829	8534307629	213736527847
		6069307408303...			
46	199	1217	9859	103069	1342907
		21219089	397681327	8682977119	217616274683
		6183541562551...			
48	223	1409	11743	125113	1656649
		26548261	503859997	11126538823	281736685679
		8081022964981...			
49	227	1433	11953	127643	1693031
		27170047	516340703	11415461989	289357897711
		8307635814431...			
50	229	1447	12097	129229	1715761
		27560453	524172379	11596829689	294145810687
		8450108859131...			
51	233	1471	12301	131707	1751411
		28171007	536433767	11881126321	301656862553
		8673774992821...			
52	239	1499	12547	134597	1793237
		28889363	550881943	12216514841	310526940547
		8938160481557...			
54	251	1597	13469	145547	1950629
		31599859	605555557	13489097663	344268078839
		9946200971687...			
55	257	1621	13709	148439	1993039
		32332763	620393003	13835380799	353471438263
		10221768670013...			
56	263	1669	14177	153877	2071583
		33691309	647927381	14478972721	370600719481
		10735307868743...			

Appendix 1

Matrix $[\overline{M}^2P]...$ Continuation 3.

57	269	1723 35368547 11374585999793...	14723 682005953	160483 15277169617	2167937 391886115431
58	271	1741 35815873 11545824668459...	14867 691097513	162257 15490445177	2193689 397580778799
60	281	1823 38235377 12479807093519...	15641 740436923	171697 16649917331	2332537 428592846379
62	293	1913 40951019 13540770614753...	16519 796000427	182261 17959785803	2487943 463728180431
63	307	2027 44432569 14919411840803...	17627 867503173	195677 19651365719	2685911 509248998611
64	311	2063 45564719 15372235794151...	17987 890830471	200017 20204583739	2750357 524169678691
65	313	2081 46082987 15580165580489...	18149 901517753	202001 20458245581	2779781 531016168117
66	317	2099 46620709 15796066509169...	18311 912598217	204067 20721384791	2810191 538121923037
68	337	2269 52286593 18099406558319...	20063 1029838717	225503 23513901553	3129913 613739626127
69	347	2341 54615469 19059563752283...	20773 1078227191	234293 24670634249	3260657 645165616243
70	349	2351 55043683 19236734782351...	20899 1087126459	235891 24883634693	3284657 650958710863
72	359	2417 57160969 20117195040149...	21529 1131224411	243781 25940205719	3403457 679722101701
74	373	2549 61460533 21922891272739...	22811 1221036307	259657 28097383163	3643579 738585245417
75	379	2609 63567289 22816010162129...	23431 1265161649	267439 29159843309	3760921 767640499331

Appendix 1

Matrix $[\overline{\mathbf{M}}^2 \mathbf{P}] \dots$ Continuation 4.

76	383	2647 64795981 23339094889519...	23801 1290918281	271939 29780778613	3829223 784640376427
77	389	2683 65864459 23795492951147...	24107 1313343397	275837 30321784529	3888551 799462887341
78	397	2719 67247771 24388288001989...	24509 1342401539	280913 31023447269	3965483 818701472243
80	409	2803 70432519 25761357737977...	25423 1409422013	292489 32644249103	4142053 863205467819
81	419	2897 73768631 27211243680073...	26371 1479780677	304553 34349423377	4326473 910115902141
82	421	2909 74172503 27387388206553...	26489 1488302867	305999 34556157661	4348681 915809403721
84	433	3019 78339559 29216297536511...	27689 1576442723	321017 36697520357	4578163 974856473813
85	439	3067 79794157 29858589333061...	28109 1607252663	326203 37447368857	4658099 995564440951
86	443	3109 81428323 30582699050611...	28573 1641908027	332099 38291437141	4748047 1018893116299
87	449	3169 83543071 31524064728311...	29153 1686826109	339601 39386748617	4863959 1049194449883
88	457	3229 85839547 32550506359429...	29803 1735649329	347849 40578571003	4989697 1082201297941
90	463	3299 88565483 33775078562347...	30557 1793681753	357473 41997140089	5138719 1121535591721
91	467	3319 89369047 34137123380603...	30781 1810798861	360293 42415879469	5182717 1133155938589
92	479	3407 92678347 35635464099689...	31667 1881428537	371981 44145738083	5363167 1181205761389

Appendix 1

Matrix $[\overline{\mathbf{M}}^2 \mathbf{P}] \dots$ Continuation 5.

93	487	3469 95121911 36747532444747...	32341 1933651711	380557 45426482839	5496349 1216826411041
94	491	3517 96797411 37512927359291...	32797 1969496239	386401 46306458839	5587537 1241322670799
95	499	3559 98330021 38214783465337...	33203 2002298621	391711 47112340151	5670851 1263771327193
96	503	3593 99630571 38811965770483...	33569 2030158657	396269 47797243919	5741453 1282861540019
98	521	3733 105089261 41333311232987...	35023 2147305243	415253 50681376121	6037513 1363360331743
99	523	3761 106166089 41833278300773...	35311 2170447637	418961 51251887327	6095731 1379303865481
100	541	3911 112073683 44591559921641...	36887 2297602183	439357 54391267121	6415081 1467155677657
102	557	4027 116881321 46855727983837...	38153 2401362767	455849 56958606937	6673993 1539140110927
104	569	4133 121064467 48838469899327...	39239 2491797367	470207 59200082443	6898807 1602086508713
105	571	4153 121834483 49204743622123...	39451 2508461203	472837 59613478459	6940103 1613705610163
106	577	4217 124469621 50460527025823...	40151 2565499711	481847 61029312569	7081709 1653521623993
108	593	4339 129647857 52942646093899...	41491 2677808011	499403 63821022049	7359427 1732128413677
110	601	4421 132814411 54468962620717...	42293 2746597487	510031 65533394977	7528669 1780407360517
111	607	4463 134389627 55230488801623...	42697 2780844971	515401 66386576369	7612799 1804479121591

Appendix 1

Matrix $[\overline{\mathbf{M}}^2 \mathbf{P}] \dots$ Continuation 6.

112	613	4517	43283	522829	7730539
		136593931	2828789699	67581794939	1838220650251
		56298481067219...			
114	619	4567	43889	530773	7856939 ...
115	631	4663	44879	543967	8066533 ...
116	641	4759	45971	558643	8300687 ...
117	643	4787	46279	562711	8365481 ...
118	647	4801	46451	565069	8402833 ...
119	653	4877	47297	576203	8580151 ...
120	659	4933	47857	583523	8696917 ...
121	661	4943	47963	584999	8720227 ...
122	673	5021	48821	596243	8900383 ...
123	677	5059	49207	601397	8982923 ...
124	683	5107	49739	608459	9096533 ...
125	691	5189	50591	619739	9276991 ...
126	701	5281	51599	633467	9498161 ...
127	709	5381	52711	648391	9737333 ...
128	719	5441	53353	657121	9878657 ...
129	727	5503	54013	665843	10020343 ...
130	733	5557	54601	673793	10147877 ...
132	743	5651	55681	688249	10382033 ...
133	751	5701	56197	695239	10493953 ...
134	757	5749	56701	702173	10606223 ...
135	761	5801	57193	708479	10707449 ...
136	769	5851	57751	715969	10829519 ...
138	787	6037	59723	742681	11261903 ...
140	809	6217	61819	771079	11723507 ...
141	811	6229	61979	773317	11760029 ...
142	821	6311	62921	786053	11967047 ...
143	823	6323	63059	788009	11999111 ...
144	827	6353	63391	792413	12071197 ...
145	829	6361	63467	793511	12089177 ...
146	839	6469	64679	809917	12356863 ...
147	853	6599	66089	828923	12667463 ...
148	857	6653	66749	838091	12816389 ...
150	863	6691	67157	843613	12907091 ...
152	881	6841	68821	866329	13280819 ...
153	883	6863	69109	870161	13343881 ...
154	887	6899	69491	875519	13431967 ...
155	907	7057	71287	900157	13836751 ...

References

- [1] *N.J.A Sloane and S. Plouffe*, "The Encyclopedia of Integer Sequences", Academic Press, San Diego, 1995
- [2] *N.J.A Sloane*, "The On-Line Encyclopedia of Integer Sequences", <http://www.research.att.com/~njas/sequences>
- [3] *L. Alexandrov*, "Multiple Eratosfhenes sieve and the prime number distribution on the plane", Sofia, 1964 (unpublished)
- [4] *Jean-Pierre Chandeux and Alain Connes*, "Conversation of Mind, Matter, and Mathematics", Princeton University Press, 2000.
- [5] *T. Forbs*, "Prime Clusters and Cunningham Chains", *Math. Comput.* **68**, pp 1739–1749, 1999
- [6] *Lubomir Alexandrov*, "On the nonasymptotic prime number distribution", math.NT/9811096 V1, LANL, Los Alamos, 1998
- [7] *F. Göbel*, "On 1–1–Correspondence between Rooted Trees and Natural Numbers", *J. of Combinatorial Theory, series B* **29**, 141–143, 1980
- [8] *A. Odlyzko, M. Rubinstein and M. Wolf*, "Jamping Champions", *Experimental Math.*, 8 (No. 2), pp 107–118, 1999
- [9] *Stein M.L., Ulam S. M. and Wells H. B.*, "A Visual Display of Some Properties of the Distribution of Primes", *Amer. Math. Monthly* **71**, 516–520, 1964
- [10] *Adolf Hildebrand and Helmut Maier*, "Irregularities in the distribution of primes in short intervals", *J. reine angew. Math.* **397**, pp 162–193, 1989
- [11] *L. Alexandrov, D. Karajov*, "Method for the Approximate Solution of Eigenvalue Problems for Linear Differential Equations of a High Order", *J. Comp. Mathem. and Mathem. Phys.*, 20, 4, pp. 923–938, 1980 (in Russian)
- [12] *Ronald L. Graham, Donald E. Knuth, Oren Patashnik*, "Concrete Mathematics", Addison–Wesley, Menlo Park, California, 1998
- [13] *A. R. Conn, N. J. H. Gould and P. L. Toint*, "Trust-Region Methods", SIAM, MPS, Philadelphia, 2000
- [14] *A. M. Odlyzko*, "Primes, quantum chaos, and computers", *Number Theory*, National Research Council (1990), pp 35–46, <http://www.dtc.umm.edu/~odlyzko/doc/zeta.html>

Received on April 17, 2002.

Александров Любомир
Последовательности и матрицы из простых чисел,
порождаемые счетными арифметическими функциями

E5-2002-55

Найден новый класс бесконечных циклических групп. В поведении простых чисел найдена закономерность, которая позволяет представить простые и натуральные числа как бесконечные матрицы с общим законом образования их рядов. Предложена нелинейная спирально-плоскостная модель арифметики вместо линейной декартовой.

Работа выполнена в Лаборатории теоретической физики им. Н. Н. Боголюбова ОИЯИ.

Сообщение Объединенного института ядерных исследований. Дубна, 2002

Alexandrov Lubomir
Prime Number Sequences and Matrices Generated
by Count Arithmetic Functions

E5-2002-55

A new class of infinite cyclic groups is found. A regularity of the behaviour of prime members is established. This regularity allows one to represent both prime and natural numbers as infinite matrices with a common formation rule of their rows. A nonlinear plane-spiral model of the arithmetic is proposed instead of the linear Cartesian one.

The investigation has been performed at the Bogoliubov Laboratory of Theoretical Physics, JINR.

Communication of the Joint Institute for Nuclear Research. Dubna, 2002

Макет *Т. Е. Попеко*

ЛР № 020579 от 23.06.97.

Подписано в печать 22.04.2002.

Формат 60 × 90/16. Бумага офсетная. Печать офсетная.

Усл. печ. л. 2,68. Уч.-изд. л. 3,66. Тираж 325 экз. Заказ № 53248

Издательский отдел Объединенного института ядерных исследований
141980, г. Дубна, Московская обл., ул. Жолио-Кюри, 6.